JOURNAL OF OPTOELECTRONICS AND ADVANCED MATERIALS Vol. 10, No. 5, May 2008, p. 1048 - 1051

Phase transformations of Co-enhanced Finemet amorphous ribbons based on resistance-temperature measurements

T. J. PAPAIOANNOU, P. SVEC[a], D. JANICKOVIC[a], C. S. KARAGIANNI, E. HRISTOFOROU[*]
[1]*National Technical University of Athens, Iroon Polytechniou 9, Athens 15780, Greece*
[2]*Slovak Academy of Sciences, Bratislava, Slovakia*

Phase transformations of $(Fe_{1-x}Co_x)_{73.5}Cu_1Nb_3Si_{13.5}B_9$ {x=0, 0.5, 1} amorphous ribbons, produced by the planar flow technique, were studied using resistance dependence on temperature (R-T) at several linear heating rates and resistance dependence on time (R-t) for isothermal heating values. Differential scanning calorimetry (DSC) measurements were also performed at 10 K/min and 40 K/min heating rates. Isothermally annealed ribbons at various temperature-time sets were investigated with XRD, showing the previous amorphous condition and the resulted crystallized material. The nanostructured grains have been observed by transition electron microscopy (TEM).

(Received March 13, 2008; accepted May 5, 2008)

Keywords: Finemet amorphous ribbons, Fe-Co-Cu-Nb-Si-B, DSC, XRD, TEM

1. Introduction

The need of more efficient soft magnetic materials led to the development of amorphous and/or nanocrystalline Fe-Cu-Nb-Si-B alloys called Finemets [1]. Since then, Finemets have been the subject of extended research regarding structural characterization, kinetics and magnetic properties [2]. Additional elements, such as Cobalt, affect the crystallization stages and the size of nano-grains in a way that has to be determined.

This article outlines the transformations occurring on a Cobalt-enriched Finemet ribbon. Measuring techniques such as R-T and R-time give interesting results regarding the temperature depended transformations. A set of DSC measurements can be a helpful tool for the interpretation of the resistance diagrams. TEM and XRD Nanocrystallization phenomena over isothermal treated ribbons can also be observed through TEM and XRD.

2. Experimental

The mother alloys were produced using a vacuum inductive furnace. The purity level of the elements was not lower than 99.5%. Ribbons were casted using the planar flow technique, over a copper wheel spinning at 30 m/s linear velocity. Ribbon dimensions were 6 mm in width and ~25 μm in thickness. Measurements regarding resistivity dependence on temperature were performed at 2.5, 5, 10, 20, and 40 K/min heating rates over the as-quenched ribbons. The accuracy of the four probe electrical arrangement reached 0.01% K for linear heating. DSC data was acquired with a Perkin Elmer 7 for 10 and 40 K/min linear heating rates. Ribbons were isothermally annealed at 773, 823, 873 and 923 K for 30 min, inside a vacuum chamber (approximately 10^{-4} torr), with an accuracy of 0.1 K. X-rays diagrams were obtained with a Siemens diffractometer. TEM preparation was realized by ion beam thinning.

2.1. Resistivity dependence on temperature

Crystallization and phase transformations of the amorphous ribbons were observed by the resistance dependence on temperature. Several heating rates were used to all three compositions. The results demonstrated phase transformations, by means of the relative resistivity value drop over temperature (K). During cooling, the resistivity values are linearly proportional to temperature from 1000 K to 300 K, clearly indicating that the crystallization process had been completed during the mentioned heating interval. A DSC diagram, regarding the same ribbon, verified the phase transformations observed by the R(T) measurements.

Regarding the pure Finemet sample ($Fe_{73.5}Cu_1Nb_3Si_{13.5}B_9$) the first crystallization was indicated by the small drop of the resistivity value approximately at 790 K, as shown in Fig. 1, depending on the heating rate, corresponding to the typical inter-metallic α-Fe_3Si DO_3 face-centered cubic phase. Higher temperatures, from ~830 to ~910 K, indicated a linear increase of relative resistivity. The changing rate of the R-values in heating and cooling had the same amplitude and opposite sign, indicating no phase transformations but only ohmic-temperature conductive dependence. For verification purposes, a DSC diagram, acquired with the same heating rates, showed that transformations are not to be expected at this area as shown in Fig. 2. The second expected transformation was revealed between ~940 and ~990 K as shown in Fig. 1. From the amorphous matrix, α-Fe_3Si, Fe_3B, $Fe_{23}B_6$ and Fe_2B were obtained.

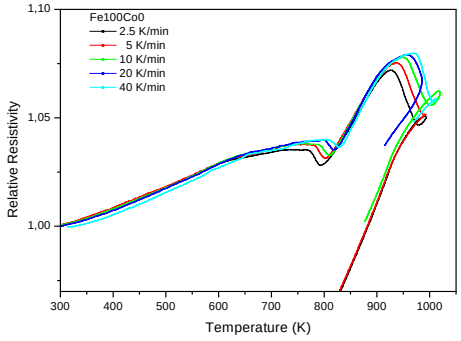

Fig. 1. R(T) for several heating rates (K/min) concerning a $Fe_{73.5}Cu_1Nb_3Si_{13.5}B_9$ ribbon.

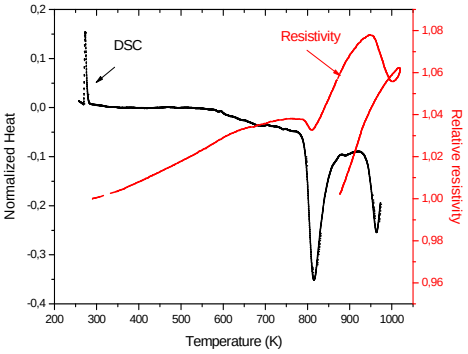

Fig. 2. R(T) in comparison with DSC for 10 K/min heating rate ($Fe_{73.5}Cu_1Nb_3Si_{13.5}B_9$) ribbon.

Concerning the $(FeCo)_{73.5}Cu_1Nb_3Si_{13.5}B_9$ composition ribbon, the crystallization process began at lower temperatures (approximately ~780 to ~880 K, as shown in Fig. 3, because of the existence of Cobalt which reduces the Glass Forming Ability [3]. The first phase obtained from this composition was fcc structures of $(FeCo)_3Si$, as verified from X-rays measurements. A noticeable drop of resistivity along 850 K indicated a decreased percentage of amorphous phase in favor of the crystalline one. The data from the DSC supports the R(T) results as shown in Fig. 4. The second drop is expected to provide the typical Finemet phases: Fe_3B, $(FeCo)_{23}B_6$ and Fe_2B.

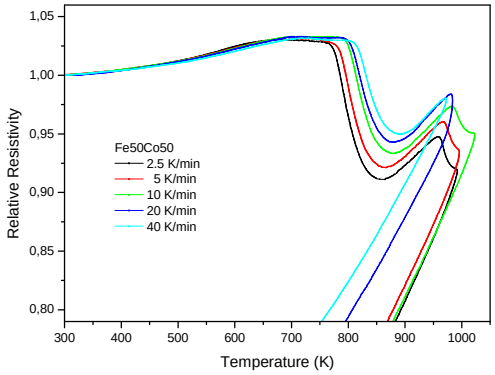

Fig. 3. R(T) for several heating rates (K/min) concerning a $(FeCo)_{73.5}Cu_1Nb_3Si_{13.5}B_9$ ribbon.

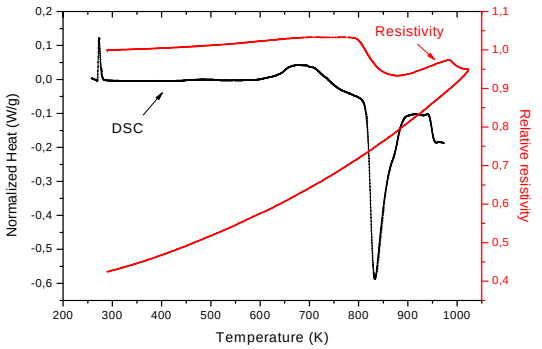

Fig. 4. R(T) in comparison with DSC for 10 K/min heating rate $(FeCo)_{73.5}Cu_1Nb_3Si_{13.5}B_9$ ribbon.

Complete substitution of Fe with Co over Finemets intrigues great interest, concerning the quantity and the quality, of the transformations occurring after linear or isothermal heating treatments. R(T) diagrams showed three distinct drops of resistivity at ~720 K, ~890 K and ~ 940 K, representing two phase transformations after first crystallization, as shown in Fig. 5. $Co_{23}B_6$ face-centered cubic phase, parallel to the growth of fcc Co crystals, follows crystallization. DSC showed a large drop upon the last transformation (Fig. 6).

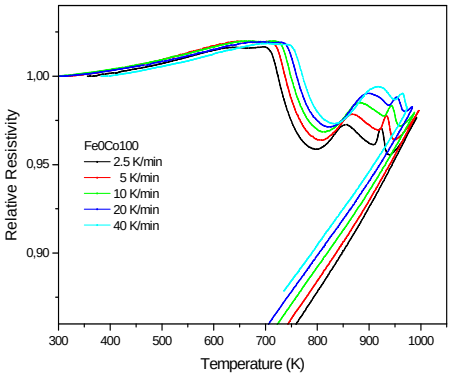

Fig. 5. R(T) for several heating rates (K/min) concerning a $Co_{73.5}Cu_1Nb_3Si_{13.5}B_9$ ribbon.

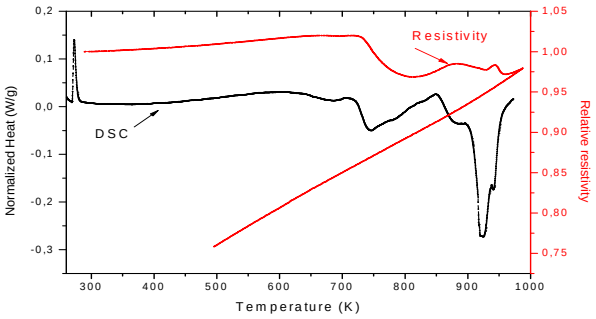

Fig. 6. R(T) in comparison with DSC for 10 K/min heating rate $Co_{73.5}Cu_1Nb_3Si_{13.5}B_9$ ribbon.

2.2. Structural characterization

XRD response of the as-quenched ribbons illustrated the presence of the amorphous phase for all three compositions. The ribbons were exposed to 773, 823, 873 and 923 K for 30 min, inside a vacuum chamber (approximately 10^{-4} torr) and the obtained XRD response indicated the crystallized phases. Fig. 7 demonstrates the evolution from the amorphous condition to the crystallized phases during isothermal heating step concerning the $Co_{73.5}Cu_1Nb_3Si_{13.5}B_9$ ribbon.

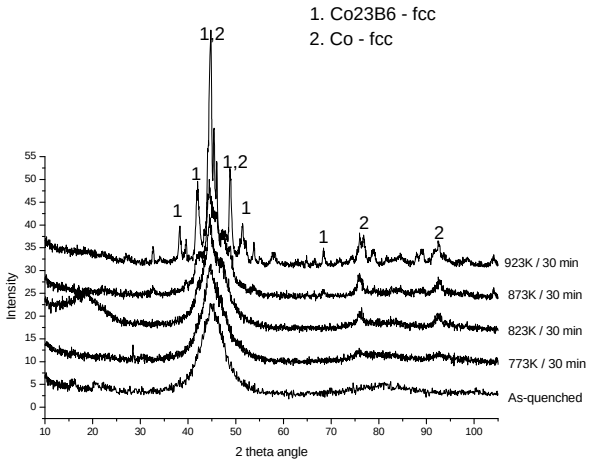

Fig. 7. Co Finemet isothermally annealed in vacuum for 30 min.

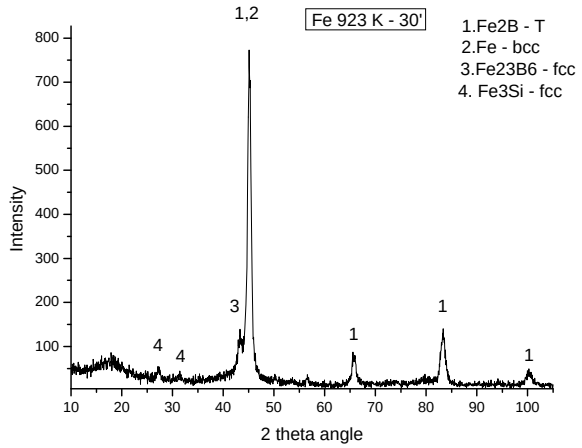

Fig. 8. Pure Finemet sample treated at 923 K for 30 min in vacuum.

TEM micrographs obtained from a Jeol Microscope (Figs. 9,10) illustrated the nano-crystalline nature of the $Co_{73.5}Cu_1Nb_3Si_{13.5}B_9$ sample. The given sample was treated at 823 K (with an accuracy reaching 0.1K) for 30 min. The size of the Co (fcc) and $Co_{23}B_6$ (fcc) nano-crystals inside the amorphous matrix varies from 5 to 20 nm. The overall amount of crystalline phase against amorphous phase does not exceed 35% of the volume at this point [5]. The crystals seem to be uniformly spread. The marks on the dark and bright field photos showed the micrographic characteristics of the $Co_{23}B_6$ phase. In the dark field photo, the phase seemed vague with no specified crystal borders and had a grey shadow at the same photo in the bright field.

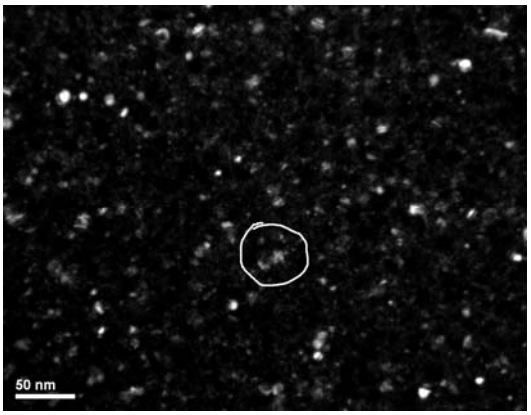

Fig. 9. Dark field micrograph illustrating the characteristics of the $Co_{23}B_6$ phase.

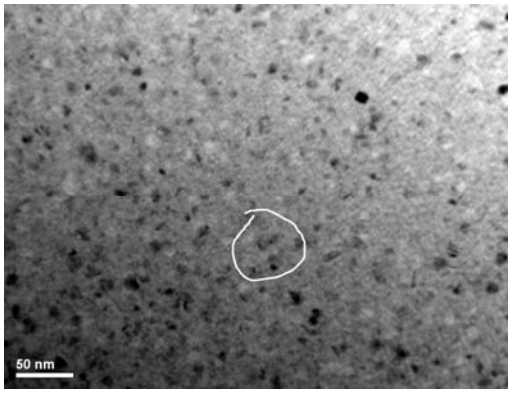

Fig. 10. Bright field micrograph illustrating the characteristics of the $Co_{23}B_6$ phase.

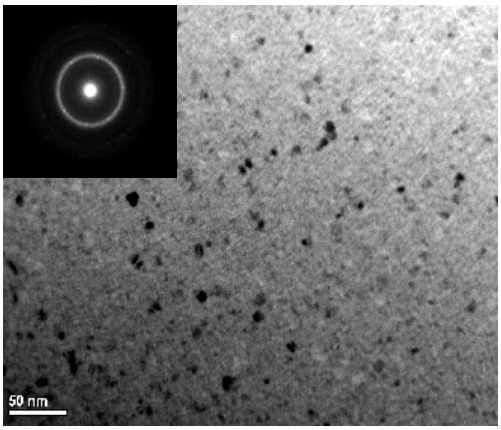

Fig. 11. TEM micrograph after thermal treatment, illustrating nano - crystallization. $Co_{73.5}Cu_1Nb_3Si_{13.5}B_9$ sample, treated at 773K for 30 min.

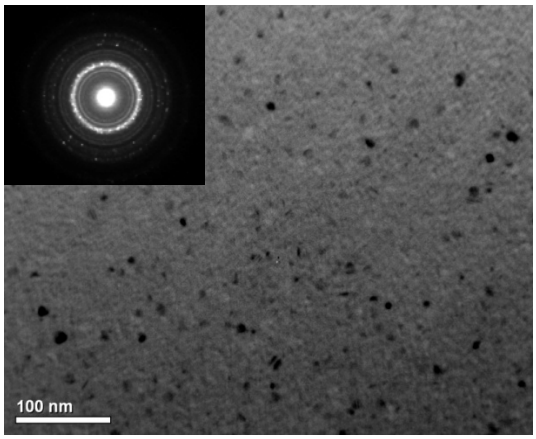

Fig. 12. $Co_{73.5}Cu_1Nb_3Si_{13.5}B_9$, treated at 823 K for 30 min.

3. Discussion and conclusions

Resistance in the tested ribbons seems to drop significantly after amorphous to crystalline transformation. Concerning pure Fe Finemet the room temperature resistance dropped about 30% for crystalline ribbons. Resistance drop is more pronounced for the case of 50% Co substitution alloys, reaching a level of 38% resistance drop, while it is more or less maintained for the complete Co substitution ribbon (35%). This observation suggests that a possible amorphous to crystalline and crystalline to amorphous phase transformation, resulting in such a significant resistance drop, may be used as the principle for non-volatile resistive random access memories cells. Accordingly, high resistivity (amorphous phase) may leaf to a bit 1, while lower resistivity (crystalline phase) may lead to a bit 0. From the experimental data it appears that the Fe-Co Finemet is the more promising composition for this purpose.

On the other hand, it is visible from resistivity measurements that resistance in the amorphous stage is quite stable with respect to temperature. This is evident for the case of the amorphous Fe-Co and Co substituted Finemet ribbons, in the order of 75 ppm/^{o}C and 60 ppm/^{o}C respectively. In the contrary, Fe rich Finemet ribbons exhibit a relatively significant dependence on temperature even in the amorphous phase, in the order of 100 ppm/^{o}C (which is also significant). Such a low temperature coefficient on resistivity changes of Co substituted ribbons may lead to the conclusion that these ribbons, in their amorphous stage, can be used as cores for magneto-resistance based field sensors. As an example they may be used as sensing cores in the recently developed field sensors using circular soft magnetic cores to determine the two-dimensional ambient field component, provided that their thickness is sufficiently small in order to allow for the precise measurement of resistance [4].

It can also be observed, from the diagrams (Fig. 1, 3 & 5) that the crystallization process holds until the temperature of approximately 700 K for the lowest heating rate, which is about 10% lower than the pure Finemet. The behavior of all three compositions corresponds to the decrease of the Glass Forming Ability [3] while substituting Fe with Co and it is to be expected that the activation energies will decrease as well. Thermodynamic calculations using the Johnson-Mehl-Avrami nucleation-growth model over resistance – time data could be the object of future research.

References

[1] Y. Yoshizawa, S. Oguma, K. Yamauchi, J Appl Phys **64**, 6044-6046 (1988).
[2] M. E. McHenry, M. A. Willard, D. E. Laughlin, Progress in Materials Science **44**, 291 – 443 (1999).
[3] C. Li, X. Tian, X. Chen, A. G. Ilinsky, L. Shi, Materials Letters **60**, 309 - 312 (2006).
[4] J. Petrou, S. Diplas, H. Chiriac, E. Hristoforou, J. Optoelectron. Adv. Mater. 1715 - 1719 (2006).
[5] M. Deanko, D. M. Kepaptsoglou, D. Muller, D. Janickovic, I. Skorvanek, P. Svec, E. Hristoforou, Journal of Microscopy 260 - 263 (2006).

* Corresponding author: eh@metal.ntua.gr